18èmes Journées Internationales de Thermique (JITH 2017)
Monastir (Tunisie), 25 - 27 Octobre 2017

CFD investigation and experimental tests of a solar dryer with thermal storage by pebble bed

Hicham EL FEROUALI*, Ahmed ZOUKIT*, Said DOUBABI*, Issam SALHI*, Toufiq EL KILALI**, and Naji ABDENOURI*
*Université Cadi Ayyad, FSTG, ER2D Marrakech, B.P 549, Morocco
**Ste CADVAL 506 Quartier Industriel 40000 Marrakech, Morocco
n.abdenouri@uca.ac.ma

Abstract: CFD studies were performed on a designed natural convection solar dryer in order to analyze the effect of the thermal energy storage by rocks. Results show that by passing hot air through rocks, these latter stores an amount of thermal energy which can be used to remedy the intermittency problem. The solar dryer was modeled in SolidWorks flow simulation in steady and transient states. Rock layers were arranged as superimposed sphere beds; each layer consists of spheres having a diameter of 3 cm. The rock layers were modeled in SolidWorks flow simulation as a porous medium. The maximum reached temperature during the sunny period and the duration of the thermal discharge phase are strongly affected by the location of rocks in the drying chamber. Experiments were carried out by using rock salt and pebbles (0.076 m^3) as thermal storage materials. These storage media have maintained the drying chamber temperature high in the absence of the solar radiation and thus, increase the drying time by 4 more hours compared to the dryer without energy storage.

Key Words: solar dryer, CFD modeling, thermal storage, pebble bed, rock salt

1. Introduction

Developing efficient and cost-effective solar dryer with thermal energy storage system has become potentially viable for drying processes in most of the developing countries [1]. The integration of thermal storage in solar dryers has to extend the drying time some hours after sunset. Over all, thermal energy can be stored as sensible heat, latent heat or chemical energy. Several designs of solar dryers with thermal storage unit have been studied over the years. These dryer systems with the thermal energy storage could mainly be classified into two types: Solar dryers that use sensible heat storage methods and the solar dryers that are based on latent heat storage methods.

Recently, many studies were focused on the phase change materials (PCMs) as storage mean in the solar dyers [2, 3, 4 and 5]. Actually, PCM has a high thermal energy storage density in contrast to sensible heat storage materials. Despite all the advantages of PCMs, sensible heat storage stills the most simple, inexpensive energy storage system and it doesn't need much maintenance [6, 7]. Dincer et al. [8] analyzed various aspects of sensible storage techniques. They observed that the selection of a sensible energy storage system depends on the economic viability and working conditions. Hence, the sensible heat storage has been identified as the main economic storage technology and much sustainable for solar drying, particularly in disadvantaged areas.

The use of pebbles or rocks for heat storage provides numerous advantages: they are non-flammable and non-toxic, cheap, and they are function as both a heat-transfer surface and a packed storage medium. Significant increase in the rate of drying was reported with the solar dryer that has pebble bed as energy storing material. Jain [9] carried out a study on a solar crop dryer with reversed absorber plate type collector. They found that thermal storage materials (Granite grits) highly affect the natural mass flow rate in the dryer. M. Mohanraj and P. Chandrasekar [10] performed an experimental study of chili drying on an indirect forced convection solar dryer equipped by the gravel as sensible heat storage materials. They found that the integration of storage materials increase the drying time by about 4 hours per day and maintain consistent the air temperature.

This paper is proposed with the following objectives:

i. To design and develop a natural convection solar dryer with thermal storage. Pebbles and Rock salts were chosen as thermal storage materials seen that they are easily available in natural areas and at low cost.
ii. To investigate the storage effect on temperature evolution in dryer chamber.
iii. To study the effect of the thermal storage on the drying chamber's temperature during the charging and discharging phases.

2. Description of the designed solar dryer

The experimental apparatus is a solar dryer composed from a solar collector which is connected to a drying chamber. The drying chamber's volume is 1 m^3 (1m x 1m x 1m), and its walls are insulated by 5 cm of mineral fiber. The solar collector's length is 2m, its width is 1 m. The absorber is made from aluminum, its top side is painted with matt black glycerophtalic lacquer that has a solar absorptivity of 0.95 and an emissivity of 0.85 [11]. The insulation in the bottom and the edges of the solar collector is insulated by 5cm thickness of mineral fiber.

3. CFD study of the solar dryer with and without energy storage

Computational fluid dynamics technique (CFD) is a perfect tool for predicting the dryer's behavior through appropriate simulation of heat and mass transfer in both gaseous and solid phases [12]. The software solves Navier-Stokes equations with the Finite Volume Method (FVM) on a rectangular (parallelepiped) computational domain which is a rectangular prism where the calculation is performed [13].

The turbulence model used in this calculation is the κ–ε model, and the turbulence parameters, such as the intensity and length turbulences and the boundary layer thickness, are calculated by default from the Reynolds number, the hydraulic diameters and the length of the walls.

The conservation laws for mass, momentum and energy in the Cartesian coordinate system could be written by respectively Eqs. (1), (2) and (3):

$$\frac{\partial \rho}{\partial t} + \frac{\partial}{\partial x_i}(\rho u_i) = 0 \qquad (1)$$

$$\frac{\partial \rho u_i}{\partial t} + \frac{\partial}{\partial x_j}(\rho u_i u_j) + \frac{\partial P}{\partial x_i} = \frac{\partial}{\partial x_j}(\tau_{ij} + \tau_{ij}^R) + S_i \qquad (2)$$

$$\frac{\partial \rho H}{\partial t} + \frac{\partial \rho u_i H}{\partial x_i} = \frac{\partial}{\partial x_j}(u_j(\tau_{ij} + \tau_{ij}^R) + q_i) + \frac{\partial P}{\partial t} - \tau_{ij}^R \frac{\partial u_i}{\partial x_j} + \rho\varepsilon + S_i u_i + Q_H \qquad (3)$$

With,

$$H = h_e + \frac{u^2}{2} \qquad (4)$$

- u: is the fluid velocity,
- ρ : is the fluid density,
- P: is the pressure,
- S_i: is a mass-distributed external force per unit mass,
- τ_{ij}: is the viscous shear stress tensor,
- τ_{ij}^R : is the Reynolds-stress tensor,
- Q_H : is a heat source or sink per unit volume,
- q_i : is the diffusive heat flux,
- ε : is the turbulent dissipation,
- h_e : is the thermal enthalpy.

The subscripts are used to denote summation over the three coordinate directions.

The following specifications are used in the CFD modeling at the software SolidWorks flow simulation:

- The solar air collector is oriented southward under an angle of 30° versus the horizontal.
- The solar dryer is performed in natural convection, so, the air inlet and outlet of the dryer are modeled by an environmental pressure of 1 atm as boundary conditions.
- The model uses the discrete ordinates (DO) radiation model.
- Gravitational effects are taken into account.
- Thermal conduction in solids is taken into consideration.

- The flow type is laminar and turbulent, laminar flows occur at low values of the Reynolds number, when the Reynolds number exceeds a certain critical value, the flow becomes turbulent.
- Solar radiation is modeled in order to be perpendicular to the glass of the solar collector.
- The wind velocity is equal to 5 m/s and its direction is 40 °C. Ambient temperature is equal to 25 °C.
- Mesh dependent study was carried out by refining the mesh until results are independent of the number of cells.
- Simulations were performed in steady and transient states. For transient state simulations, the time steps were automatically determined by the software; in all cases, they are less than 0.15 s.

3.1. Simulation of the solar dryer in natural convection without storage medium

A transient simulation was performed on the dryer without storage medium (Figure 1). In this part, the considered solar radiation has a flux of 900 W/m^2 between 0 and 30 min, then, it has a value 0 W/m² between 30 min and 60 min (Figure 2). Figure 3 shows the average temperature of the air in the drying chamber as a function of time. After deactivation of the solar radiation at t = 30 min, the temperature decreases from 77 °C until it reaches 27 °C at t = 60 min. Hence, in 30 min, the temperature decreases by 50 °C and becomes almost equal to the ambient temperature. The experimental study carried out on the dryer without storage material confirms this trend. In order to maintain high temperature, even after deactivation of the solar radiation, heat storage medium was introduced into the drying chamber.

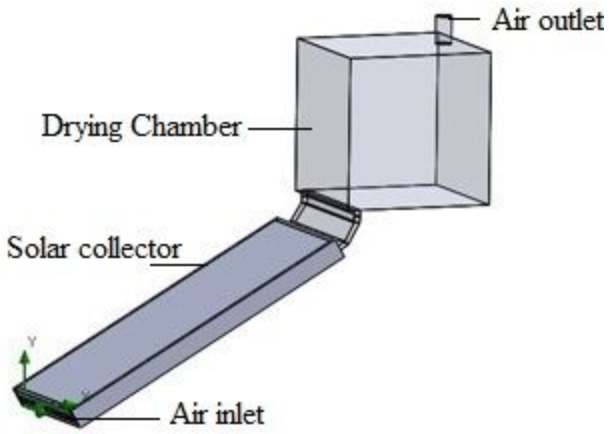

Figure 1: Simulated solar dryer without adding storage medium

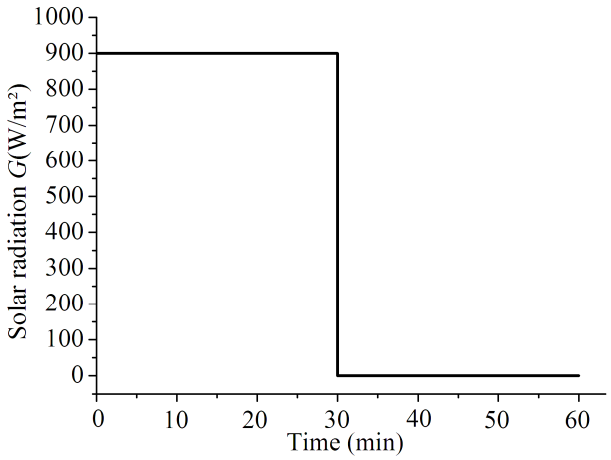

Figure 2: Solar radiation as a function of time

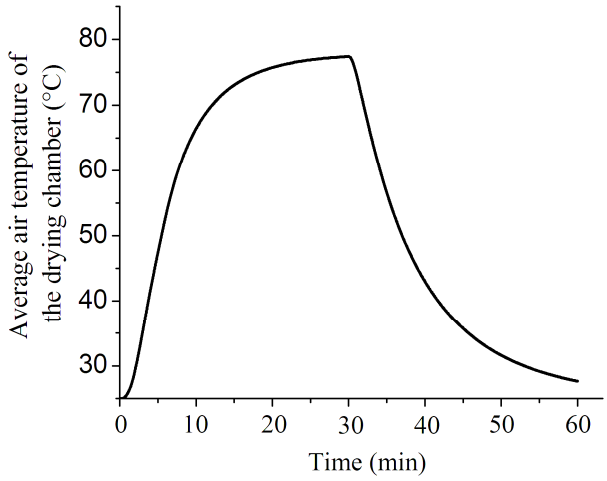

Figure 3: Average air temperature in the drying chamber as a function of time for the dryer without storage medium

3.2. Simulation of the solar dryer in natural convection with the addition of layers of rocks

3.2.1. Modeling of rock layers

Rock layers were arranged as superimposed sphere beds; each layer consists of spheres having a diameter of 3 cm. To simplify the calculations, each rock layer was modeled in SolidWorks flow simulation by a porous medium.

3.2.2. Calculation of the properties of the porous medium

The effective porosity of the porous medium is defined as the volume fraction of the interconnected pores divided by the total volume of the medium as given by Eq (5). It is equal to 0.48 for sphere layers.

$$\varepsilon = \frac{V_{pores}}{V_{totale}} \qquad (5)$$

Permeability of the storage medium is isotopic, so it does not depend on the direction of the air in the medium. For the resistance of the porous medium k, it is formulated by Eq (6):

$$k = -\frac{grad(P)}{\rho V} = \frac{\Delta P.S}{\dot{m}L} \qquad (6)$$

Where P, ρ, V are respectively the pressure, the density and the velocity. ΔP is the pressure difference between the opposite sides (Figure 4) of a parallelepiped porous body, $\dot{m}$ is the mass flow through the body, S and L are consequently the area of the cross-section and the length of the body, all in the selected direction.

Figure 5 show the evolution of the pressure difference ΔP between the opposite sides as a function of the mass flow. In fact, a simulation was performed for 4 rocks positioned inside a wind tunnel, the length of the body L and the cross section S are equal in this case respectively to 0.03 m² and 0.0036 m².

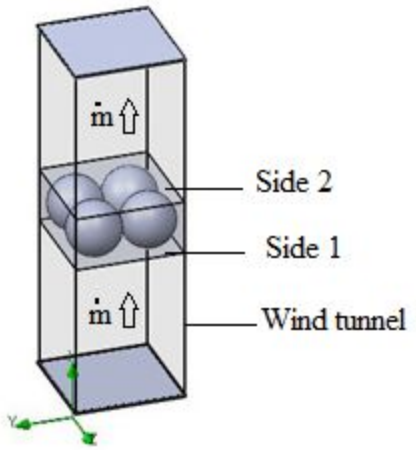

Figure 4: Wind tunnel to determine the parameters specifying the coefficient of resistance

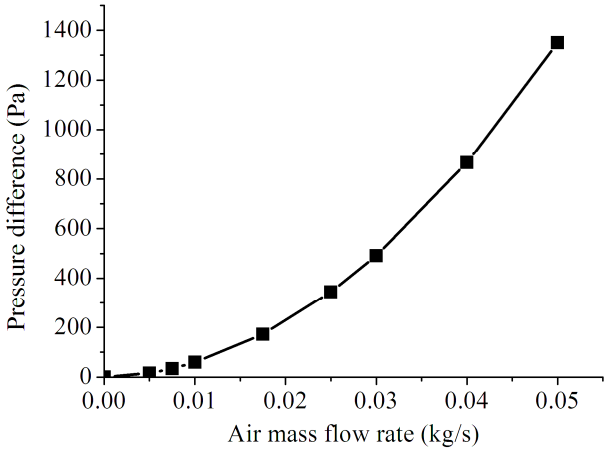

Figure 5: Pressure difference as a function of the air mass flow rate (kg/s)

Fluid heat exchange indicates how to define the heat exchange between the fluid and the porous matrix; it is defined by the heat exchange coefficient and specific area. The volumetric heat exchange coefficient is calculated as following:

$$\gamma = h\frac{S_{pores}}{V} \qquad (7)$$

Where h is the heat exchange coefficient between the inner surface of the porous body and the fluid h=10W/m².K.
S_{pores}/V is the specific area of the porous body, i.e., the inner surface area of the solid matrix of this porous body, per unit volume V of the porous body. It is equal to 104.71 m^{-1}.
The thermo-physical properties of the storage medium used in the CFD study are presented in Table 1:

Table 1: Thermo-physical properties of the storage medium used in the CFD study

Thermo-physical property	Value
Porosity	0.48
Density (kg/m^3)	2600
Specific calorific capacity (kJ/kg.K)	0.828
Melting temperature (°C)	1200
Thermal conductivity (W/m.K)	3

3.2.3. Positioning of the rocks in the drying chamber

Two positions of storage materials were considered:

- Case 1: Three layers of superimposed porous medium were simulated; the positioning is shown in Figure 6a and Figure 7a. The total volume of the porous media is 0.076 m^3.
- Case 2: Six layers of superimposed porous medium were simulated according to the positioning shown in Figure 6b and Figure 7b. The total volume of the porous media is the same to the first case (0.076 m^3).

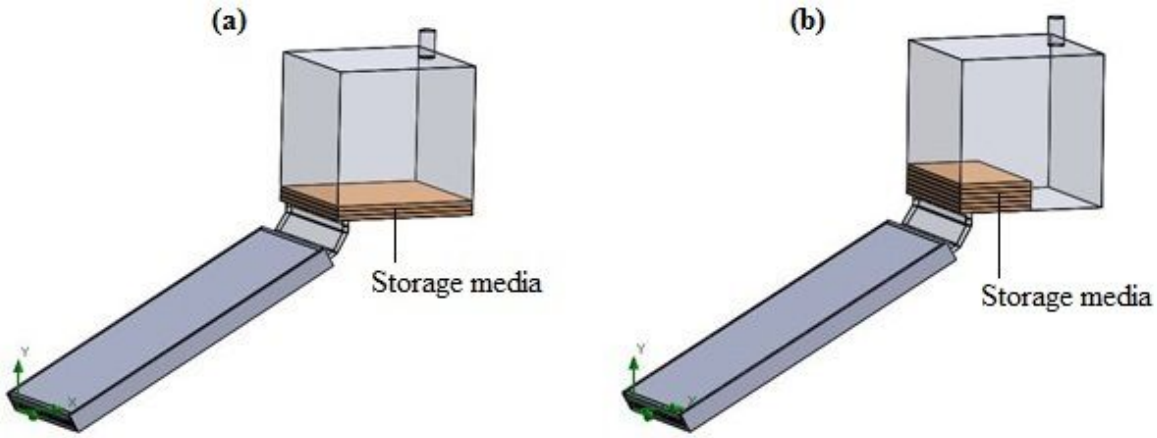

Figure 6: Perspective view of rocks positioning in the solar dryer: a) case 1, b) case 2

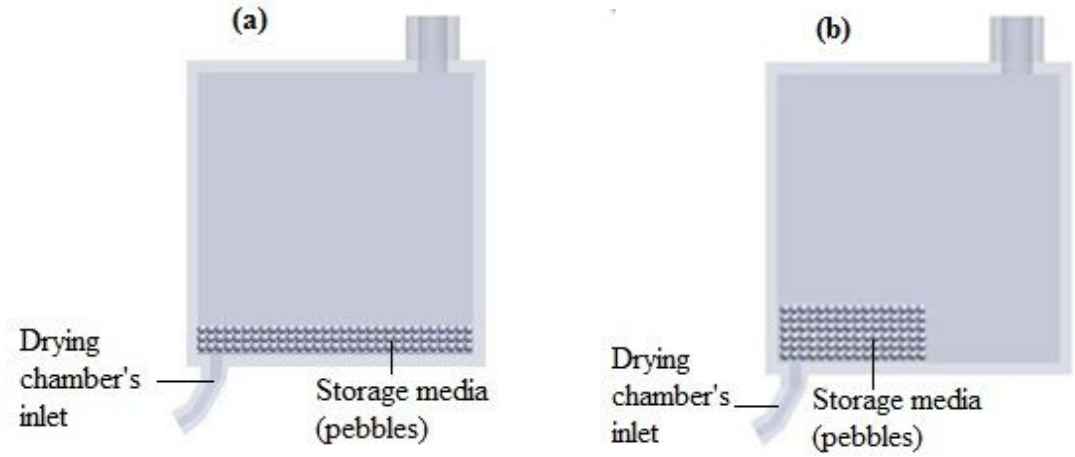

Figure 7: Cross section view of rocks positioning in the drying chamber: a) case 1, b) case 2

Figure 8 shows the simulations of the temperature distribution inside the dryer in steady state at a constant solar flux of 900 W/m² and for an ambient temperature of 25°C. By comparing of the two storage configurations, it could be noted that in the first case, only the part of storage medium located at the chamber entrance allow the heat storage. Far from this entrance, and just near the middle, the temperature of storage medium drops from an average of 95 to 58 °C. In the second set, the temperature distribution of the storage medium is higher (between 80 and 98 °C). Hence, almost all the rocks allow the heat to be stored in. This last case seems to be more suited for thermal storage.

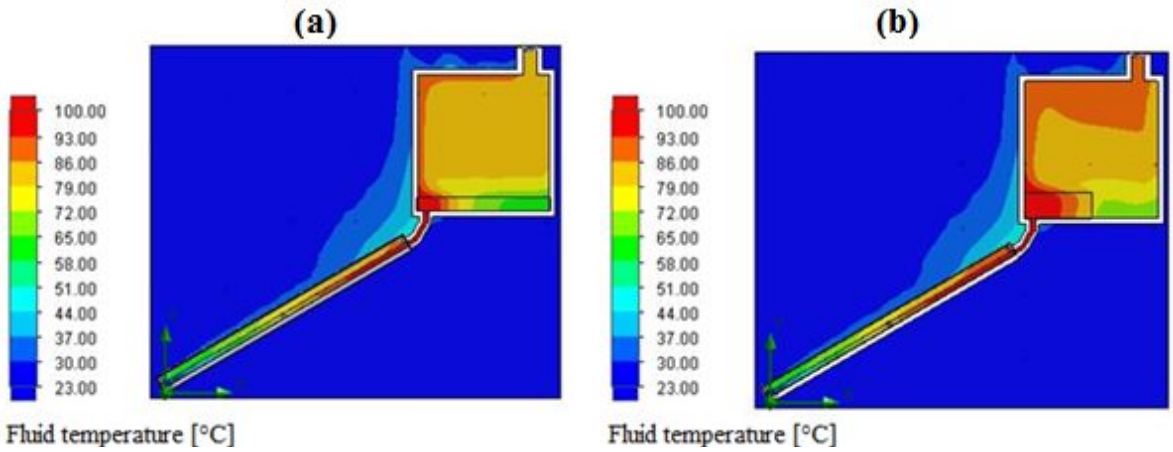

Figure 8: Transversal view of the fluid temperature distribution a) case 1, b) case 2

Transient simulation was performed on the solar dryer with storage medium positioned according to case 1. For a solar radiation profile on which this last has a value of 900 W/m² from t = 0 min to t = 30 min then it is canceled, the temperature reaches 50 °C after 30 min of operation at a solar radiation of 900 W/m² (Figure 9), After stopping of the solar radiation, the temperature decreases to 35 °C at t = 60 min. So, the temperature drops by 15 °C after 30 min, then it reaches the ambient temperature after almost 1h 38 min.

In contrast to case 1 in which the mean drying chamber temperature reached 50 °C after 30 min, this latter reached in case 2 a temperature of 50 °C only after 90 min at the same solar radiation of 900 W/m^2 (Figure 9). After 30 min of deactivation of the solar radiation, the temperature drops only by 6 °C, and it reaches the ambient temperature after almost 5 h 30 min.

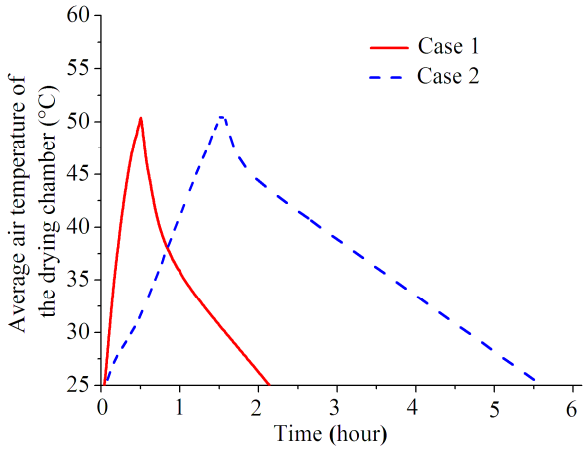

Figure 9: Average air temperature in the drying chamber as a function of time for the dryer without storage, and with storage according to cases 1 and 2

4. Experimental tests

Experiments were carried out on March 2017 in Marrakech (Morocco). The solar dryer was kept in shadow before beginning the experiment in order to cancel the solar effect on the temperature of the dryer's components. The dryer was then exposed to solar radiation from 10 h 45 min to 12 h 15 min (GMT), and then the solar collector is covered until the difference between the ambient temperature and the drying chamber temperature become almost equal to 6 °C. During experiments, the ambient temperature, and the drying chamber's temperature were measured every 15 minutes by PT100 kimo TM110 temperature sensor. The storage medium temperature was measured by PT100 kimo SFC 50 temperature sensor. The solar radiation was also measured by a Kipp & Zonen SMP10 pyranometer at 30° inclined plan. The air velocity at the outlet of the dryer was measured by Kimo CTV210.

Three experiments were carried on the solar dryer (see Table 2). Exp. 1 was performed without the integration of energy storage, Exp. 2 and Exp. 3 were carried out on the solar dryer with respectively rock salt and pebbles as storage media. The rocks were arranged according to case 2. The total volume of the storage

medium is almost 0.076 m^3, (0.91m x 0.465m x 0.18m), thermo-physical properties are presented in Table 3 for rock salt and pebbles. The specific calorific capacities were measured by calorimetry.

The porosity are almost 0.36 and 0.42 respectively for rock salt and pebbles. Pebbles and rock salt are available in Morocco especially at TENSIFT, NFISS and TASSOUT rivers for pebbles, and in TELOUET and DARAA for rock salt.

Table 2: Experimental tests' details

Experimental test	Details
Exp. 1	Dryer without storage medium
Exp. 2	Dryer with rock salt as storage medium
Exp. 3	Dryer with pebbles as storage medium

Table 3: Thermo-physical parameters

Thermo-physical property	Rock Salt	Pebbles
Density (kg/m^3)	2200	2600
Specific calorific capacity (kJ/kg.K)	0.92	0.828
Melting temperature (°C)	800.4	1200

Figure 10 represents the measured solar radiation and ambient temperature during Exp. 1, Exp. 2 and Exp. 3. Mean solar radiations that are received by the solar dryer between 10 h 45 min and 14 h 15 min GMT (charging phase) are 926, 1062 and 1030 W/m² respectively for Exp. 1, Exp. 2 and Exp. 3. Then, the solar collector is covered by opaque cover in order to analyze the dryer's behavior at the absence of solar radiation and the effect of the storage media on the drying chamber temperature (discharging phase). The air flow rate was measured during the experiments, its average values are equal during the charging phase to 30.25, 24.91 and 27.52 m^3/h, and they are equal during the discharging phase to 25.10, 13.88 and 13.68 m^3/h for respectively Exp. 1, Exp. 2 and Exp. 3. Hence, the integration of storage media decreases the air flow rate by almost 18 % and 9.02 % respectively for rock salt and pebbles during the charging phase, and by about 44.7 % and 45.5 % respectively for rock salt and pebbles during the discharging phase. Consequently, the charge loss is more substantial for the discharging phase by the addition of storage media.

According to Figure 11, For Exp. 1, the drying chamber temperature is higher during the charging phase than Exp. 2 and Exp. 3 on which storage media are used. But during the discharging phase, For Exp. 1 the drying chamber temperature drops fast and becomes superior to the ambient temperature by 6°C after just 2 h 15 min of disabling solar radiation. By the addition of rock salt (Exp. 2) or pebbles (Exp. 3), the drying chamber temperature drops and becomes superior to ambient temperature by almost 6 °C after 6 h 15 min. Hence the addition of rock salt and pebbles as storage media maintains the drying chamber temperature high and could increase the drying time by 4 more hours compared to the dryer without energy storage.

During the charging phase, the temperature of rock salt and pebbles increase and then get stable at a maximum temperature between 80 and 90 °C (Figure 12), then its temperature decrease during the discharging phase and transfer heat to the inlet air flow. The ratio of the total power stored by the rock salt and pebbles on the mean power received from the sun are calculated by the following formula:

$$\eta(\%) = 100\frac{mCp(T_f - T_i)/\Delta t}{G_{av}S} \qquad (8)$$

In which:

- m: is the mass of the storage media, it is equal to 60 kg for rock salt and to 86 kg for pebbles
- Cp: is the specific calorific capacity (KJ/Kg.K)
- T_f: is the final temperature of the storage medium at the end of the experiment
- T_i: is the initial temperature of the storage medium at 14h15min when the dryer stops receiving solar radiation
- G_{av}: is the mean value of solar radiation from 10h45min to 14h15min
- S: is the solar collector aperture area, It is equal to 2m²

This studied ratio is equal to 6.25 % for rock salt and to 8 % for pebbles, hence pebbles are higher than rock salt in terms of the stored energy regarded to the received energy by the solar dryer.

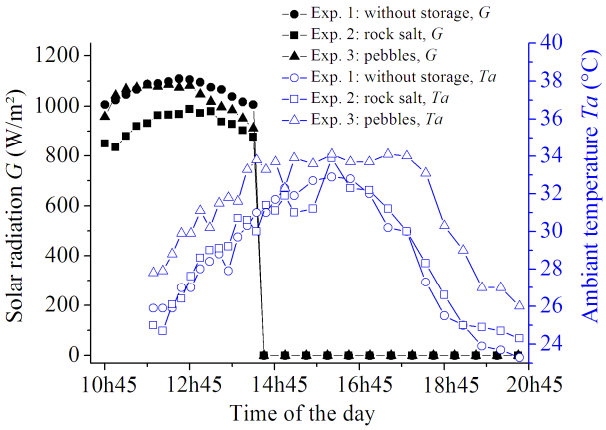

Figure 10: solar radiation and ambient temperature versus time

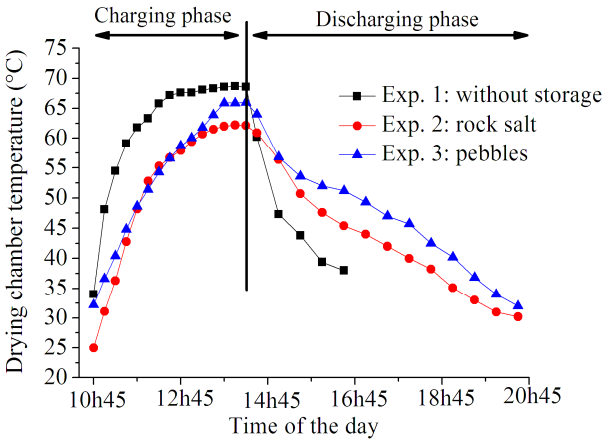

Figure 11: Drying chamber temperature of Exp. 1, Exp. 2 and Exp. 3

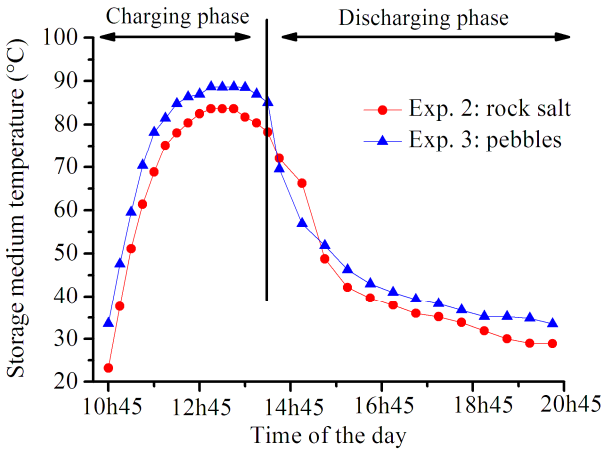

Figure 12: storage medium temperature

Conclusion

For the simulation of the solar dryer without storage medium, the temperature reached 77 °C after 30 min at a solar radiation of 900 W/m² and it drops quickly to attain the ambient one just 30 minutes after stopping incident radiation. In the other hand, by loading the bottom of the drying chamber by storage medium, the temperature rises to 50 °C after 30 min at a solar radiation of 900 W / m². Then, the temperature drops just by 15 °C after 30 min of the deactivation of solar radiation (loading configuration case 1). Another improvement was made by changing the pebble bed position inside the drying chamber (loading configuration case 2). It is

observed that this last configuration leads to maintain the temperature after enabling solar radiation, as well as it dropped only by 6 °C after 30 min. But in this case, the temperature reached 50 °C only after 90 min at a solar radiation of 900 W / m².

Three experiments were carried on the solar dryer: without the integration of energy storage and with respectively rock salt and pebbles as storage media. This storage media maintain the drying chamber temperature high and could increase the drying time by 4 more hours compared to the dryer without energy storage.

The ratio of the total power stored by the rock salt and pebbles on the mean power received from the sun by the dryer were calculated. It is equal to 6.25 % for rock salt and to 8 % for pebbles, hence pebbles are higher than pebbles in terms of the stored energy regarded to the received one.

The obtained results aims to strengthen studies carried out on controlling and managing energy in the solar thermal devices. Furthermore, it will improve the efficiency of solar devices by the hybridization of the energy sources.

Acknowlegement

This work was supported by the research institute for solar energy and new energies (IRESEN) as part of the project SSH and all of the authors are grateful to the IRESEN institute for its cooperation.

References

[1] BAL, Lalit M., SATYA, Santosh, and NAIK, S. N., Solar dryer with thermal energy storage systems for drying agricultural food products: a review. Renewable and Sustainable Energy Reviews, vol. 14, no 8, p. 2298-2314, 2010.
[2] Devahastin, S., &Pitaksuriyarat, S., Use of latent heat storage to conserve energy during drying and its effect on drying kinetics of a food product, Applied Thermal Engineering, vol. 26, p. 1705-1713, 2006.
[3] Jain, D., &Tewari, P., Performance of indirect through pass natural convective solar crop dryer with phase change thermal energy storage, Renewable Energy, vol. 80, p. 244–250, 2015.
[4] Sain, P., Songara, V., Karir, R., &Balan, N., Natural convection type solar dryer with latent heat storage, In Renewable Energy and Sustainable Energy (ICRESE), 2013 International Conference on IEEE, p. 9-14, 2013.
[5] Dina, S. F., Ambarita, H., Napitupulu, F. H., & Kawai, H., Study on effectiveness of continuous solar dryer integrated with desiccant thermal storage for drying cocoa beans, Case Studies in Thermal Engineering, vol. 5, p. 32–40, 2015.
[6] Anderson R, Bates L, Johnson L, Morris JF, Packed bed thermal energy storage: a simplified experimentally validated model, J Energy Storage vol. 4, p. 14–23, 2015.
[7] Barrientos MAI, Sobrino C, Ibanez JAA, Modeling and experiments of energy storage in a packed bed with PCM, Int J Multiph Flow, vol. 86, p. 1–9, 2016.
[8] Dincer I, Dost S, Li X. Performance analysis of sensible heat storage systems for thermal applications. Int J Energy Res vol. 21, no. 12, p. 1257-1171, 1997.
[9] Jain, D., Modeling the performance of the reversed absorber with packed bed thermal storage natural convection solar crop dryer, Journal of Food Engineering, vol. 78, no. 2, p. 637–647, 2007
[10] Mohanraj, M., &Chandrasekar, P., Performance of a forced convection solar drier integrated with gravel as heat storage material for chili drying, Journal of Engineering Science and Technology, vol. 4, no. 3,p. 305–314, 2009.
[11] Henninger, J. H., Solar Absorptance and Thermal Emittance of Some Common Spacecraft Thermal-Control Coatings (No. NASA-RP240400-1121). NATIONAL AERONAUTICS AND SPACE ADMINISTRATION WASHINGTON DC, 1984.
[12] Chen, H.H.; Huang, T.C.; Tsai CH, Mujumdar, A.S., Development and performance analysis of a new solar energy-assisted photocatalytic dryer, Drying Technology, vol 26, no. 4, p. 503-507, 2008.
[13] MATSSON, John E. An Introduction to SolidWorks Flow Simulation 2013. SDC publications, 2013.